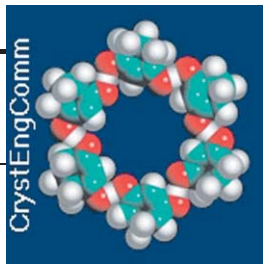

Paper

Fingerprinting intermolecular interactions in molecular crystals†

Mark A. Spackman* and Joshua J. McKinnon

Chemistry, University of New England, Armidale, NSW 2351, Australia.
E-mail: mspackma@metz.une.edu.au

Received 2nd April 2002, Accepted 17th May 2002
Published on the Web 18th July 2002

We have recently described a remarkable new way of exploring packing modes and intermolecular interactions in molecular crystals using a novel partitioning of crystal space. These molecular Hirshfeld surfaces reflect intermolecular interactions in a novel visual manner, offering a hitherto unseen picture of molecular shape in a crystalline environment. The surfaces encode information about all intermolecular interactions simultaneously, but sophisticated interactive graphics are required in order to extract the information most efficiently. To overcome this we have devised a two-dimensional mapping which summarizes quantitatively the nature and type of intermolecular interaction experienced by a molecule in the bulk, and presents it in a convenient graphical format. The mapping takes advantage of the triangulation of the Hirshfeld surfaces, and plots the fraction of points on the surface as a function of the closest distances from the point to nuclei inside and outside the surface. In this manner all interaction types (for example, hydrogen bonding, close and distant van der Waals contacts, C–H$\cdots\pi$ interactions, π–π stacking) are readily identifiable, and it becomes a straightforward matter to classify molecular crystals by the nature of interactions, and to rapidly identify similarities and differences which can become obscured when examining crystal packing diagrams. These plots are a novel visual representation of all the intermolecular interactions simultaneously, and are unique for a given crystal structure and polymorph. Applications to a wide variety of molecular crystals and intermolecular interactions are presented, including polymorphic systems, as well as crystals where $Z' > 1$.

Introduction

A recurring theme in very recent publications concerned with intermolecular interactions in solids, and especially crystal engineering, is the increasing impetus for a means of considering jointly all interactions between molecules, rather than the historical focus on selected close atom–atom contacts. In their wonderful monograph on weak hydrogen bonds,[1] Desiraju and Steiner note, "There is a growing need to simultaneously assess different interactions and to establish their hierarchy". Even more directly relevant to the present work is a statement by Nangia and Desiraju,[2] and it is worthwhile quoting a paragraph from the section of that work entitled *Comparison of Crystal Structures*. This section makes the point that a full understanding of crystal packing and design require a treatment of the entire molecule and all interactions. "Given such realities, an immediate need in crystal engineering is to be able to compare crystal structures. Many will appreciate that the structure of, say, naphthalene resembles that of anthracene more than it resembles benzene. Is it possible to quantify such comparisons? If so, such quantification would amount to pattern matching and becomes important because crystals that are structurally similar are also likely to have similar properties. Ideally, one would like to arrive at an index of similarity between two crystal structures. In order that two or more structures are deemed to be similar or dissimilar, two steps are involved: (1) identification of the core structural features; and (2) evaluation of the extent of their likeness."

In our recent work we have developed a tool which specifically addresses these objectives. It is based on Hirshfeld surfaces,[3] which themselves provide a remarkable new way of exploring packing modes and intermolecular interactions in molecular crystals using a novel partitioning of crystal space. We have demonstrated elsewhere[4] that molecular Hirshfeld surfaces reflect intermolecular interactions in a novel visual manner, offering a hitherto unseen picture of molecular shape in a crystalline environment. The surfaces encode information about all intermolecular interactions simultaneously, but sophisticated interactive graphics are required in order to extract the information most efficiently. For example, we have explored in some detail the colour mapping of a variety of functions on the surfaces, including distance from the surface to the nearest nucleus outside the surface, as well as functions of the principal curvatures of the surface. Examples can be provided in virtual reality, but publication of such results remains uncommon. Although we are convinced that these interactive graphical representations offer insight into intermolecular interactions in crystals, which nicely complements tools such as crystal packing diagrams and those available through the Cambridge Structural Database (CSD),[5] they are nevertheless restricted to the laboratory. To overcome this limitation we have devised a two-dimensional mapping which summarizes quantitatively the nature and type of intermolecular interactions experienced by a molecule in the bulk, and presents it in a convenient graphical format. The mapping takes advantage of the triangulation of the Hirshfeld surfaces, and plots the fraction of points on the surface as a function of the closest distances from the point to nuclei inside and outside the surface. In this manner interactions are readily identifiable, and it becomes a straightforward matter to classify molecular crystals by the nature of interactions, and to rapidly identify similarities and differences which can become obscured or difficult to identify when examining crystal-packing diagrams.

These 2D plots are a novel visual representation of all the intermolecular interactions simultaneously, and are unique for a given crystal structure and polymorph. In this paper we introduce these 'fingerprint' plots, and provide numerous

†Based on the presentation given at CrystEngComm Discussion, 29th June–1st July 2002, Bristol, UK.

 DOI: 10.1039/b203191b

applications to a wide variety of molecular crystals and intermolecular interactions, including polymorphic systems, as well as crystals with more than one molecule in the asymmetric unit ($Z' > 1$).

Description of the method

As described elsewhere,[3,4] Hirshfeld surfaces are defined implicitly by the simple equation $w(\mathbf{r}) = 0.5$, where the weight function $w(\mathbf{r})$ is given by

$$w(\mathbf{r}) = \sum_{i \in \text{molecule}} \rho_i(\mathbf{r}) / \sum_{i \in \text{crystal}} \rho_i(\mathbf{r})$$

where $\rho_i(\mathbf{r})$ is a spherical atomic electron distribution located at the ith nucleus. The weight function represents the ratio between the sum of spherical atom electron densities for a molecule (the *promolecule*) and the same sum for the entire crystal (the *procrystal*), and therefore the Hirshfeld surface envelops that region of space surrounding a particular molecule in a crystal where the electron distribution of the promolecule exceeds that due to any other molecule.[6] In practice, a typical Hirshfeld surface is represented by tens of thousands of surface points obtained by triangulation, and two parameters convey information about relevant contact distances from each point (Fig. 1):

d_i distance from the surface to the nearest atom *interior* to the surface;

d_e distance from the surface to the nearest atom *exterior* to the surface.

To construct a 2D fingerprint plot the molecular Hirshfeld surface is first obtained using standard methods.[7] Fig. 2 provides an example of such a graph for formamide, along with Hirshfeld surfaces with d_i and d_e mapped upon them. The Hirshfeld surfaces display quite clearly two close intermolecular contacts to the carbonyl oxygen atom (red circles on the d_e surface), a double hydrogen bond acceptor, and a single close distance d_i near one of the N–H hydrogen atoms; the other hydrogen bond donor is hidden in this orientation. The majority of both of these surfaces are coloured green (representing neither close nor distant contacts), and remaining features are blue corresponding to longer contact distances. There is clearly valuable information on intermolecular interactions encoded on both surfaces, and to gain a more complete appreciation of all interactions simultaneously it is necessary to refer to both distances for each point, a non-trivial process for 3D objects such as these.

To overcome this difficulty d_i and d_e are calculated for each surface point, and the data are binned into discrete intervals of d_i and d_e.[8] Each point on the 2D-graph (Fig. 2) represents a bin

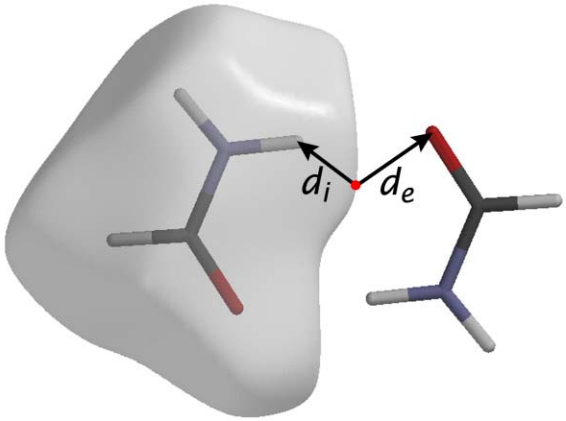

Fig. 1 Centrosymmetric hydrogen-bonded dimer of formamide in the crystal. The Hirshfeld surface of the molecule on the left is shown in transparent mode, and the distances d_i and d_e illustrated schematically for a single point (red dot).

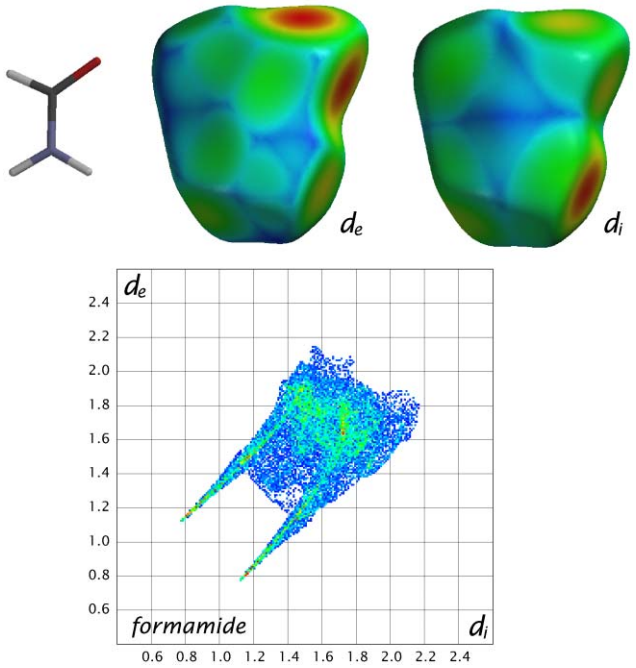

Fig. 2 Hirshfeld surfaces for formamide (FORMAM02) with d_e (left) and d_i (right) mapped in colour (in both cases red represents the closest contacts, and blue the most distant contacts). The 2D fingerprint plot produced from these two functions is presented below.

of width 0.01 Å in these two distances, and the colour of each point is a function of the fraction of surface points in that bin, ranging from blue (relatively few points) through green (moderate fraction) to red (many points).[9] We display this 2D-graph as a grid of coloured points, usually over the range 0.4–2.6 Å in each of d_i and d_e.

The most obvious characteristics of these plots are their pseudo-symmetry about the diagonal where $d_i = d_e$, the relatively limited range of the points (none are found at very long or very short distances), the rather uniform colouring (indicating that most combinations of d_i and d_e occur with much the same frequency in this crystal), and the two sharp features pointing to the bottom left of the plot. The pseudo-symmetry of the plots is a direct consequence of the close packing of the Hirshfeld surfaces, which guarantees that where surfaces touch one-another (and provided that there is only one molecule in the asymmetric unit) both of the points (d_i, d_e) and (d_e, d_i) will appear on the 2D-graph. As a consequence, the lower of the two sharp features in Fig. 2 corresponds to the hydrogen bond acceptor (where $d_i > d_e$) and the other to the hydrogen bond donor (where $d_e > d_i$). Similarly, because Hirshfeld surfaces are smooth and leave small voids where no single molecule dominates the procrystal electron density, not all parts of the surfaces are touching, and for points in these regions of the surface d_e is generally greater than d_i.

Before presenting detailed examples of these fingerprint plots, we note that a related 2D-graph for displaying intermolecular interactions has already been described, although applications to date appear to be limited. We refer here to the so-called NIPMAT (Nonbonded Interaction Pattern MATrix) plots,[10] which display for every pair of atoms in a molecule the deviation of shortest intermolecular contacts from the sum of their van der Waals radii. The result for an N-atomic molecule is an $N \times N$ matrix presented as gray scale pixels, with the gray tone ranging from black (very short contacts) through shades of gray to white (very long contacts). To our knowledge the only published examples of such matrices are for naphthalene and terephthalic acid,[11] 2-, 3-, and 4-aminophenol,[2] and 1,4-benzoquinone and fluoranil.[1,12] NIPMAT has also been employed to examine the near equivalence of predicted

structures of uracil, 6-azauracil and allopurinol by Price and Wibley,[13] and an attempt was made to apply it to the polymorphism of a steroidal sapogenin.[14] The latter work on a relatively large molecule ($C_{27}H_{40}O_5$) highlighted one of the limitations of NIPMAT, namely the size-dependence of the resulting matrix. In addition, NIPMAT plots are not unique for any given molecular crystal; they depend on the chosen ordering of atoms in constructing the $N \times N$ matrix, and there are many reasonable choices that can be made. As we demonstrate below, the present fingerprint plots are unique for any molecule in any molecular crystal, and their size is independent of the number of atoms in the molecule.

Examples of key interactions

There are many ways of classifying intermolecular interactions in molecular crystals, and to a certain extent the definition of various categories is somewhat arbitrary. We make use of a relatively simple classification scheme here because the nomenclature is becoming increasingly common, especially in the crystal engineering literature, and also because it lends itself rather nicely to a hierarchical parade using our 2D fingerprint plots. The scheme we employ is that described in various articles, and sometimes with changing nomenclature, by Desiraju. In his classic 1989 monograph,[15] Desiraju classified intermolecular interactions into four broad types, and these were presented in four separate chapters: Structures Based on Mostly van der Waals Forces (Ch. 4); Some Structures Based on Hydrogen Bonding (Ch. 5); Structures Based on Intermolecular Contacts to Halogen Atoms (Ch. 6); and Structures Based on Intermolecular Contacts to Sulfur (Ch. 7). This classification was slightly updated and modified in 1996,[16] and recently Desiraju and Steiner have presented a clearer rationale for distinguishing between various types of hydrogen bonds.[17] However, recognising that in most compounds of interest more than one, and often all, of these identifiable interactions contribute to the ultimate stability of the crystal, we have not slavishly followed this classification in what follows. Instead, we focus on families of molecules, with the objective of identifying characteristic patterns which emerge in the 2D fingerprint plots, and which can be unambiguously assigned to individual interaction types. Wherever possible we have chosen the same groups of molecular crystals which have been the subject of recent crystallographic investigations, with the expectation that in this manner (*i.e.* by referring back to the original publications and the methods used therein) we will be able to demonstrate more convincingly the enormous potential of this simple graphical tool.

Aliphatic hydrocarbons

There is little doubt that the dominant interactions in crystals of aliphatic hydrocarbons are isotropic and dispersive in nature, and the crystal structures are largely explained in terms of simple close-packing ideas. Nevertheless, there are still a number of interesting aspects to supposedly straightforward structures such as those of the *n*-alkanes. Boese and co-workers have recently reported X-ray structures of *n*-propane to *n*-nonane,[18] with the aim of addressing the well-known alternation of melting points and the anomalously low melting point observed for *n*-propane.[19] Those workers analysed the packing of the *n*-alkanes in terms of a simple geometrical model involving close packing of polygons, trapezoids and parallelograms.

Fig. 3 presents 2D fingerprint plots for the *n*-alkanes from ethane to *n*-nonane. The plots depict only H···H contacts, and are characterised by a relatively small range in both d_i and d_e (in both cases the majority of points lie between 1.2 and 1.8 Å). The shortest contact in all cases is quite clearly very close to 1.2 Å, the generally acknowledged van der Waals radius for hydrogen.[20] Even a cursory glance at Fig. 3 suggests that not all *n*-alkanes produce the same 2D graphs, and there are identifiable similarities and differences. Even in these simple structures these plots serve to 'fingerprint' the intermolecular contacts in the crystal by their type and by their relative frequency. Ethane, propane, butane and pentane display features which are all recognisably different from one another, while the plots for hexane and octane are virtually identical, as are those for heptane and nonane. This pattern quite nicely reflects the different space groups and crystal structures for the lower members of this series, and the similar structures and identical space groups for hexane upwards.

We can explore these plots in further detail as it is possible to correlate several of their most obvious features with short and long intermolecular contacts within the crystal. The red stripe roughly along the diagonal reflects a large fraction of points on the Hirshfeld surfaces that involve nearly head-to-head H···H contacts (*i.e.* a nearly linear C–H···H–C orientation) between neighbouring molecules. This feature is evident in all plots in Fig. 3, although it is not as pronounced for *n*-pentane, and is practically absent for *n*-propane. The plot for *n*-propane is in fact quite different from those of the other alkanes, not just in the area mentioned, but also in regions where d_i or d_e are greater than 1.8 Å. The dotted nature of the plot in these regions reflects a relatively small number of points, but these are at quite large distances from any H nuclei, and arise from long H···H contacts between the ends of *n*-propane molecules in the crystal; in effect the terminal methyl groups are adjacent to more 'empty' space than is the central methylene group. This feature hints at the reason for the unexpectedly low melting point of *n*-propane, and it is the same conclusion reached earlier by Boese and co-workers.[18]

A similar feature (*i.e.* a substantial number of points where d_i or d_e are greater than 1.8 Å) distinguishes the heavier odd-members (*n*-heptane and *n*-nonane) from the even-members (*n*-hexane and *n*-octane). Inspection of the Hirshfeld surfaces reveals that, as for propane, these features arise from points surrounding the terminal methyl groups in these molecules. These 2D-graphs are quite clearly identifying an important difference between even and odd members of this series and, most importantly, isolating that difference to the less-dense packing around the ends of the molecules. Again, Boese and co-workers have discussed this previously, but we believe it is most striking in the present fingerprint plots.

Finally, in light of its much narrower plot in Fig. 3, and a rather obvious short head-to-head H···H contact (the rather narrow feature at the bottom left of the plot, converging at $d_i + d_e = 2.36$ Å) a few comments on the structure of *n*-butane are warranted. The structure used in constructing the plot in Fig. 3 is from Boese and co-workers (DUCKOB04), obtained from the disordered high-temperature phase at 90 K. As described in the original paper, the disorder could not be adequately resolved in the structural analysis, which resulted in a relatively high value of $R_1 = 19.2\%$, and hence the fingerprint plot for *n*-butane in Fig. 3 is best regarded as tentative.[21]

Fig. 4 displays fingerprint plots for cyclohexane, and the tetragonal polymorph of adamantane, and these clearly show exactly the same essential features observed for the *n*-alkanes in Fig. 3. Slight differences can be seen in the displacement of the whole pattern to shorter contacts, suggesting a more dense packing for these heavier molecules. In addition, adamantane displays a long blue tail, with $d_e > 2.2$ Å for some points, a distance considerably greater than any observed for the *n*-alkanes. This feature can be identified with the methylene groups, all of which point towards a small cavity in the crystal.

Fingerprint plots for ethylene and acetylene (Fig. 5) are remarkably different from that for ethane (Fig. 3), and show a number of new features, the most striking being the presence of 'wings' at top left and bottom right of each plot. This feature can be readily identified as a result of C–H···π interactions

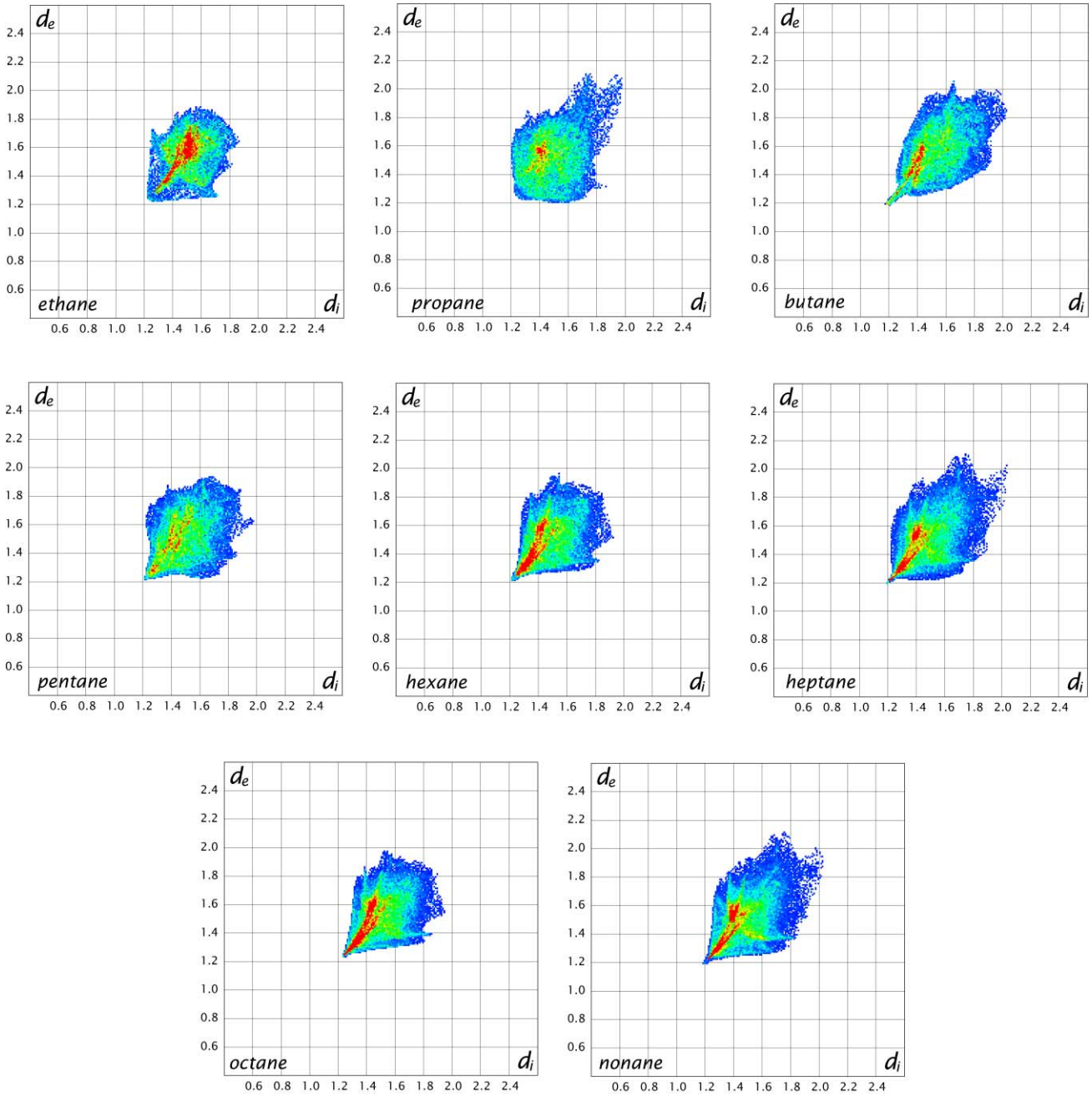

Fig. 3 2D fingerprint plots for the *n*-alkanes: ethane (ETHANE01), propane (JAYDUI), butane (DUCKOB04), pentane (PENTAN01), hexane (HEXANE01), heptane (HEPTAN02), octane (OCTANE01) and nonane (QQQFAY01).

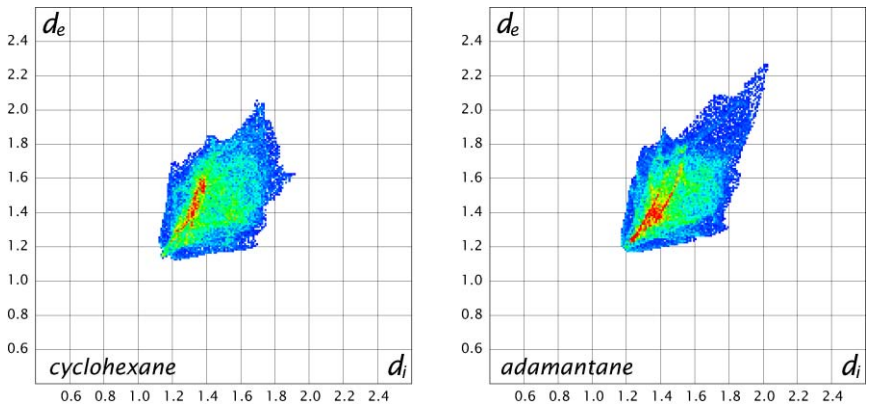

Fig. 4 2D fingerprint plots for cyclohexane (CYCHEX05) and adamantane (ADAMAN08).

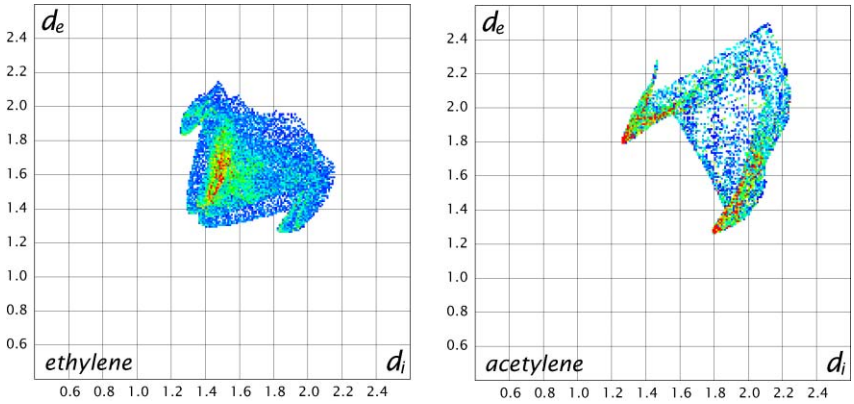

Fig. 5 2D fingerprint plots for ethylene (ETHLEN10) and acetylene (ACETYL02).

in both crystals, and it appears with regularity for aromatic hydrocarbons in the following section. The wing at the top left ($d_i < d_e$) corresponds to points on the surface around the C–H donor, whereas that at the bottom right ($d_e < d_i$) corresponds to the surface around the π acceptor, in this case the double or triple carbon–carbon bond. The remainder of the plot for ethylene is strikingly reminiscent of those for the *n*-alkanes, although with no very close H···H contacts evident, while the absence of any similarity between the plot for acetylene and those for the *n*-alkanes suggests no H···H contacts at all for this species. Instead, the intermolecular contacts in acetylene are overwhelmingly C–H···π (either as donor or acceptor, as evidenced by the red colouring of both of the 'wings'); remaining points on the Hirshfeld surface are small in number (judging by the sparseness and colour of the dots) and can be rationalised in terms of small cavities which result from the closest packing of these small, rod-like molecules.

Polycyclic aromatic hydrocarbons

We choose this class of compounds partly because of the remark by Nangia and Desiraju quoted in the Introduction, partly because they have been studied previously as a group by others,[22,23] and also because they contain interactions ('aromatic' interactions, C–H···π and π···π) which are receiving increasing attention in supramolecular and biological chemistry, and are still the object of detailed attempts to understand their origin and structural consequences.[24] Our interest here is not in understanding their nature, but rather to explore how our fingerprint plots may aid in rationalising the various interactions they exhibit, and for this purpose we make use of the classification scheme proposed by Desiraju and Gavezzotti.[22]

Fig. 6 presents 2D fingerprint plots for several polycyclic aromatic hydrocarbons (see Chart 1 for molecular structures), and it is immediately obvious that these plots differ substantially from those for the *n*-alkanes (Fig. 3). Most evident is the greater spread of points – the 2D plots for these aromatic hydrocarbons typically cover much greater ranges in both d_e and d_i (from 1.0 Å to almost 2.6 Å in Fig. 6), and we attribute this to the presence of several different (and anisotropic) interactions, as well as the dramatically anisotropic shape of these molecules.

The plot for benzene is least like that of the other molecules in the figure. It shows a closest H···H contact of approximately 2.5 Å (*i.e.* where $d_e = d_i \approx 1.25$ Å), not unusually short, but most importantly it displays the 'wings' at the upper left and lower right that we now recognise as characteristic of a C–H···π interaction. For benzene these features are sharp and exceptionally well defined, a consequence of the highly symmetric contact in this case (the C–H proton lies almost exactly above the ring centroid). The only other feature worth commenting on for benzene is the substantial number of points at large d_e and d_i, the blue tails at the top right of the plot. Careful inspection reveals that there are three distinct envelopes of points in this region, and they correspond to three regions on the Hirshfeld surface without any close contacts to nuclei in adjacent molecules, in much the same way as observed already for acetylene.

Naphthalene exhibits features that are similar in some ways to benzene, especially the 'wings' due to C–H···π interactions. Although there are two such contacts in naphthalene, one close and one considerably more distant, only one shows up in the plot and because it is aligned off the centre of a 6-ring, this characteristic feature is now blurred. There are differences which are equally obvious, including the presence of a closer head-to-head H···H contact (the pointed feature on the diagonal at the bottom left), and the complete absence of points at the upper right. As it turns out, there is a much more striking resemblance to the 2D plot for anthracene, although the latter has one more C–H···π interaction, leading to the distinct sawtooth shape on the lower right of the plot for anthracene. From these plots it is very clear that "the structure of … naphthalene resembles that of anthracene more than it resembles benzene". We note that according to Desiraju and Gavezzotti,[22] benzene, naphthalene and anthracene are examples of 'herringbone' structures, and in their plot of interplanar angle *versus* short axis (Fig. 3 in ref. 22) it is significant that benzene is a distinct outlier for this structural type.

Other herringbone structures included in Fig. 6 are phenanthrene (IV in Chart 1) and triphenylene (V) and, as expected, their fingerprint plots closely resemble those for naphthalene and anthracene, especially that of phenanthrene. Triphenylene displays a significant additional feature, one that is completely absent in the other herringbone structures. This is the blue-green area centred at $d_e = d_i \approx 1.8$ Å, close to the van der Waals radius of carbon,[20] and it arises from the appearance of a significant overlap between parallel triphenylene molecules, the onset of π···π stacking in this series. Again, we note that triphenylene also appears as an outlier in the plot presented by Desiraju and Gavezzotti, and it might be better regarded as belonging to the γ structure type (see below).

Pyrene (VI in Chart 1), an example of a 'sandwich herringbone' structure, where dimeric pairs pack in herringbone fashion, also exhibits a similar feature to triphenylene at 1.8 Å, although it is more marked in this case. The plot for pyrene also shows the presence of several C–H···π contacts, as well as an anomalously short (and very real[23]) head-to-head H···H contact near 2.0 Å. Perylene (VII) also forms a sandwich herringbone structure, and its 2D plot in Fig. 6 is closely similar to that for pyrene. An important difference between the two occurs in the region of the wings due to C–H···π contacts. The crystal packing for perylene results in eight identifiable contacts

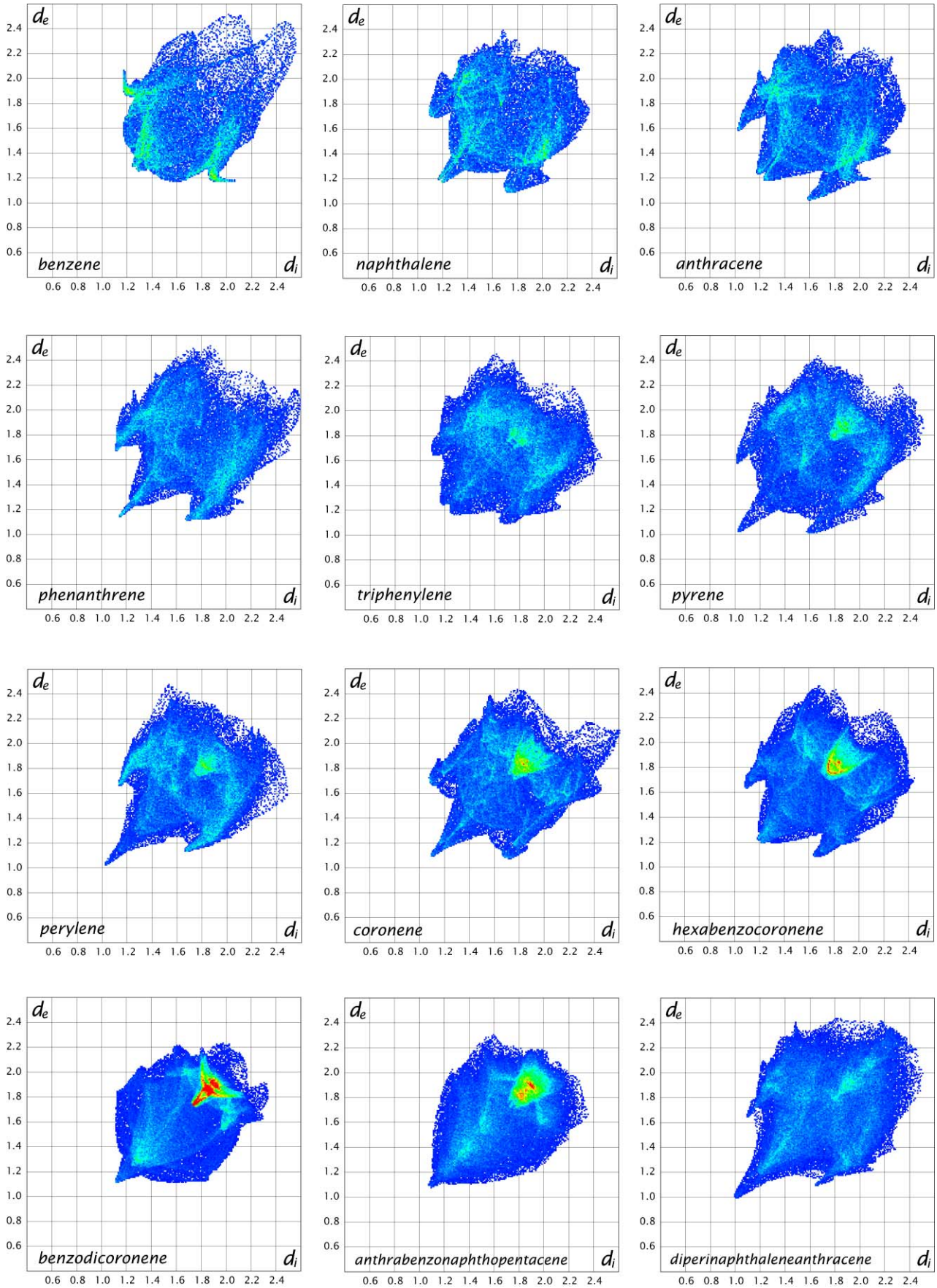

Fig. 6 2D fingerprint plots for polycyclic aromatic hydrocarbons: benzene (BENZEN07), naphthalene (NAPHTA10), anthracene (ANTCEN10), phenanthrene (PHENAN13), triphenylene (TRIPHE11), pyrene (PYRENE02), perylene (PERLEN04), coronene (CORONE), hexabenzocoronene (HBZCOR01), benzodicoronene (YOFCUR), anthrabenzonaphthopentacene (BOXGAW01), and diperinaphthaleneanthracene (NAPANT01).

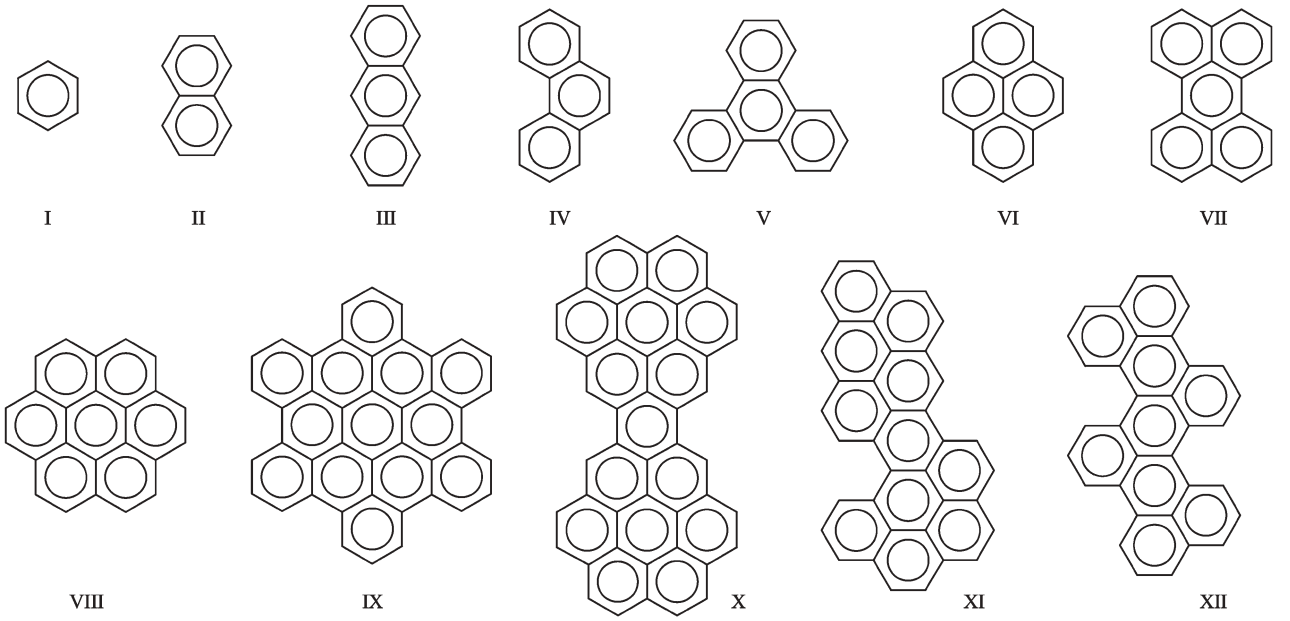

Chart 1 Structures of polycyclic aromatic hydrocarbons in Fig. 6: benzene (I), naphthalene (II), anthracene (III), phenanthrene (IV), triphenylene (V), pyrene (VI), perylene (VII), coronene (VIII), hexabenzocoronene (IX), benzodicoronene (X), anthrabenzonaphthopentacene (XI), and diperinaphthaleneanthracene (XII).

of this kind compared with four (two close and two distant) for pyrene, and for this reason the relevant feature in Fig. 6 is no longer dark blue, but blue-green, indicating that a greater proportion of points on the Hirshfeld surface involves contacts of this kind. Perylene also clearly exhibits an exceptionally short H···H contact near 2.0 Å, although this molecule was not included in the study by Dunitz and Gavezzotti,[23] and hence not mentioned in that work.

Coronene (VIII) and hexabenzocoronene (IX) are examples of the γ structure type of Desiraju and Gavezzotti, described in that work as a "sort of flattened out herringbone". Fig. 6 illustrates this rather nicely, with the 2D plots for these molecules displaying features due to C–H···π contacts, but also an increasing proportion of π···π stacking contacts – the region near 1.8 Å on the diagonal is now yellow to red – facilitated by the flattening of the herringbone motif.

The fourth structural classification of Desiraju and Gavezzotti, the β structure, possesses a layer structure, composed mostly of 'graphitic' planes (*i.e.* layers with a plane-to-plane overlap closely approximating that in graphite). Examples in Fig. 6 are benzodicoronene (X in Chart 1) and anthrabenzonaphthopentacene (XI), and it is readily apparent that their fingerprint plots are markedly different from those of the other structure types – and rather beautiful. The 'wings' due to C–H···π contacts are absent in both plots, and what was a subtle feature near 1.8 Å is now red and considerably extended, especially in benzodicoronene. The dominant contact between molecules is now clearly π···π stacking, along with H···H contacts between the edges of these large molecules, and we expect that a detailed analysis of the region between 1.7 and 2.0 Å for benzodicoronene would demonstrate that the plane-to-plane stacking is characteristic of graphite, rather than offset as in coronene and hexabenzocoronene. We note that the difference between 2D plots for these two molecules is largely due to the twisted nature of anthrabenzonaphthopentacene (XI), induced by repulsion between H atoms at the entrance to the re-entrant part of the molecule (bottom left in Chart 1). The final fingerprint plot in Fig. 6 is for diperinaphthaleneanthracene (XII), also classified as a β structure by Desiraju and Gavezzotti.[22] However, the fingerprint plot is dissimilar from those of the other two β structures in the figure, and quite clearly shows features characteristic of all the above structure types (π···π stacking, C–H···π, H···H, and even a very close H···H contact). This molecule is actually considerably twisted from planarity, again induced by intramolecular H···H repulsions (see Chart 1), and this prevents the crystal packing from achieving an arrangement that optimises the (anticipated) dominant π···π stacking interaction. The appearance of a considerable number of points beyond 2.3 Å is further evidence of 'cavities' in the structure, and hence non-optimal packing.

Although we have presented 2D fingerprint plots for only a dozen polycyclic aromatic hydrocarbons, we have demonstrated quite convincingly that this simple tool provides a rapid visual means of discriminating between the various structure types, summarizing in a concise fashion the various interactions and their relative occurrence in a given structure, and even pinpoints examples where molecules such as triphenylene and diperinaphthaleneanthracene exhibit features characteristic of more than one structure type.

Hydrogen bonding

Hydrogen bonding is without doubt the most important intermolecular interaction encountered in molecular crystals, and its classification, nature, description and structural implications have been the subject of a vast literature. Of relevance to crystal engineering, especially within the context of the present work, are various monograph chapters,[25] the book by Desiraju and Steiner,[1] as well as a very recent review article by Steiner.[26] For the presentation of results in this section it is tempting to employ the classification in Table 1.6 of ref. 1, which distinguishes between strong and weak donors, as well as strong and weak acceptors. However, we have already encountered examples of the weak donor/weak acceptor type (C–H···π), and in constructing 2D fingerprint plots for other typical hydrogen bonds it became clear to us that it is usually impossible to classify molecular crystals by a single interaction type. Instead, we follow Desiraju again, and focus on molecules with specific functionality, and the topological hydrogen-bonded patterns that emerge from a number of these simple supramolecular synthons. We make no attempt to be comprehensive, and we restrict our attention to what are currently regarded as 'conventional' hydrogen bonds.

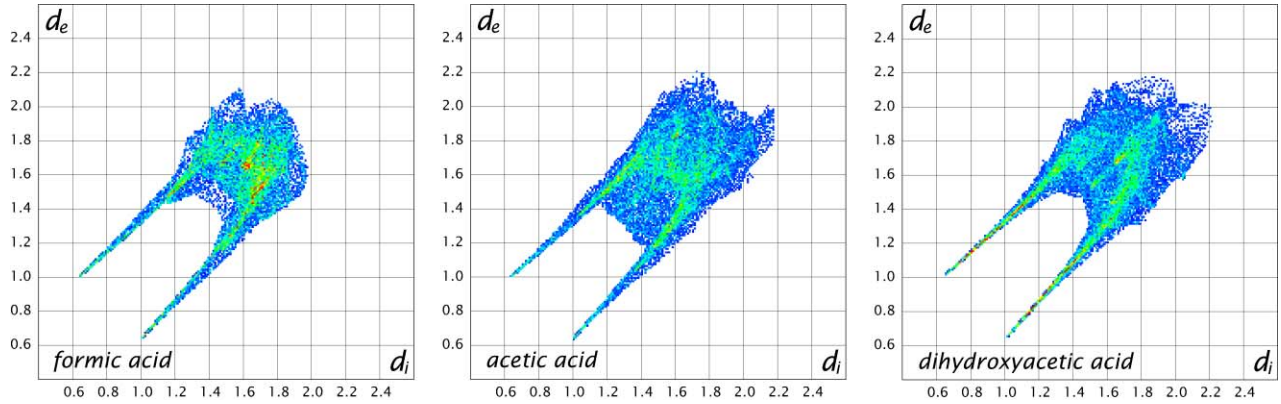

Fig. 7 2D fingerprint plots for formic acid (FORMAC02), acetic acid (ACETAC03) and dihydroxyacetic acid (CAFMIF).

Carboxylic acids

It is now well established that carboxylic acids RCO_2H form two types of hydrogen-bonded patterns – dimers and catemers – depending on the size of the R functional group. Fig. 7 presents examples of 2D fingerprint plots for catemer-forming structures. All three show the pattern characteristic of hydrogen bonding observed for formamide in Fig. 2: two sharp features pointing to the lower left of the plot, the upper one corresponding to the H-bond donor, and the lower one to the acceptor. In all cases the shortest contact is nearly identical, and close to 1.65 Å (*i.e.* the minimum value of $d_e + d_i$ is 1.65 Å), typical of O–H···O=C hydrogen bonding. Careful inspection of Fig. 7 and crystal packing diagrams reveals that the longer C–H···O=C contact is also superimposed on the hydrogen bond features for formic acid; this is seen in the thickening of the sharp features near $(d_i, d_e) = (1.5, 1.2)$, corresponding to the closest C–H···O=C contact near 2.6 Å in the crystal structure of this compound. The plot for acetic acid contains an additional feature, namely a substantial number of points between the sharp features, representing close contacts between 1.2 and 1.4 Å in both $d_e + d_i$. These points correspond to a close contact between methyl H atoms at a shortest distance of *ca.* 2.6 Å. The plot for dihydroxyacetic acid does not contain this feature, and in fact summarizes features from a large number of O–H···O=C hydrogen bonds. In this structure the carbonyl oxygen accepts hydrogen bonds only from alcohol O–H groups, and all O–H groups in the molecule are involved in hydrogen bonds. As a consequence the sharp H-bond features in the plot are no longer blue, but contain a number of orange and red points, evidence that a greater fraction of surface points are involved in close H-bond contacts in this crystal structure.

Fig. 8 illustrates 2D plots for carboxylic acids that form centrosymmetric dimers in the crystal, and a casual inspection reveals a significant difference between these plots and those in Fig. 7. Here we see that in each case there is a rather diffuse collection of points between the sharp H-bond features, with a shortest contact near 2.3 Å. This pattern derives from a small number of surface points, namely those on the surface which divides the centrosymmetric hydrogen-bonded 6-ring between the two molecules, and they arise from very close contacts between H···H and O···O across the ring. Although the crystal structure of benzoic acid (XIII in Chart 2) is actually disordered with two possible orientations of the centrosymmetric dimer, we have chosen an ordered arrangement for the purposes of constructing a 2D plot. The plot in Fig. 8 reveals a close O–H···O=C hydrogen bond contact, and the blue-green area centred at (1.9, 1.9) results from the stacking between dimers, which is not π···π in character but rather the benzene rings of one dimer lie above, and offset from, the carboxylate group of another. The diffuse pattern of blue spots at distances greater than 2.2 Å is reminiscent of that observed for benzene (Fig. 6) and their origin is also similar. The crystal structure of terephthalic acid (XIV) also includes a longer C–H···O contact (superimposed on the conventional O–H···O=C features) as well as stacking between planar ribbons of molecules hydrogen bonded at each end. As expected from the discussion above on aromatic hydrocarbons (and see, for example, the plot for coronene in Fig. 6), this π···π stacking motif shows up as a distinct red spot near $d_e = d_i \approx 1.8$ Å. Propionic acid (XV) clearly does not contain an interaction of this kind, but its plot does display the pattern characteristic of aliphatic H···H contacts (Fig. 3), superimposed on that for O–H···O=C hydrogen bonds.

Amides

The functionality of the amide group is in many ways similar to that of carboxylic acids, except that the substitution of NH_2 for OH provides an additional H-bonding capacity, which leads to a greater diversity of structures. Nevertheless, as for

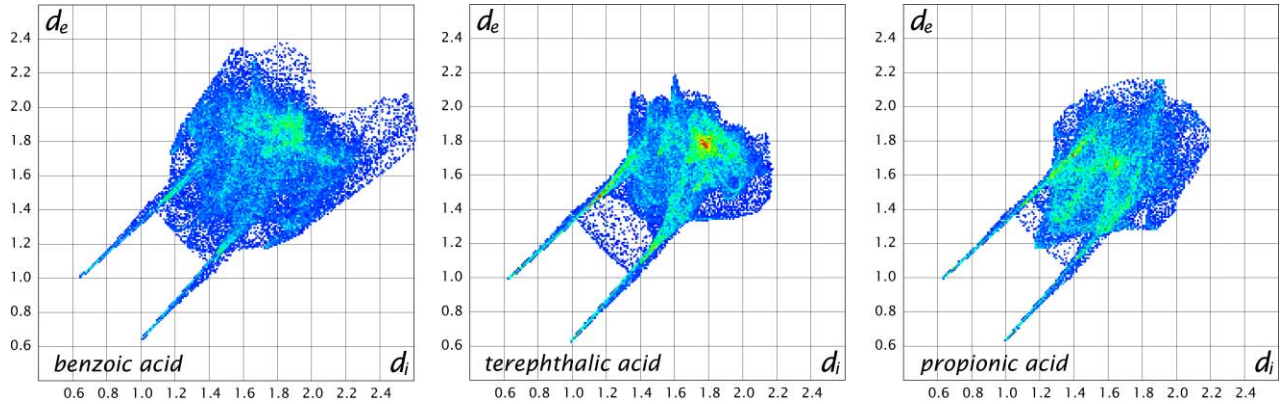

Fig. 8 2D fingerprint plots for benzoic acid (BENZAC02), terephthalic acid (TEPHTH03) and propionic acid (PRONAC).

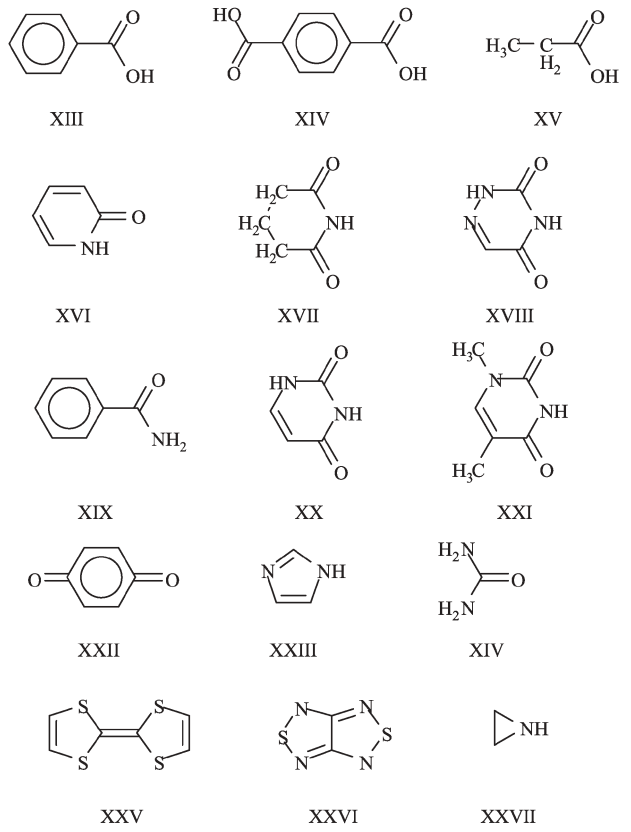

Chart 2 Structures of less-common molecules in Figs. 8, 9, 10, 11, 14 and 17: benzoic acid (XIII), terephthalic acid (XIV), propionic acid (XV), 2-pyridone (XVI), glutarimide (XVII), 6-azauracil (XVIII), benzamide (XIX), uracil (XX), 1-methylthymine (XXI), 1,4-benzoquinone (XXII), imidazole (XXIII), urea (XIV), tetrathiafulvalene (TTF) (XXV), dithiadiazole (XXVI), aziridine (XXVII).

carboxylic acids, there are still two main motifs – dimers and chains – and Figs. 9 and 10 provide examples of each. The plot for 2-pyridone (Fig. 9; XVI in Chart 2) displays three characteristic patterns: the single N–H···O=C hydrogen bond extending down to (d_i, d_e) = (0.7, 1.1) (corresponding to a H-bond distance of 1.8 Å), a relatively close H···H contact just short of 2.4 Å, and the 'wings' typical of a C–H···π contact, which in this case approaches 2.7 Å, similar to that in naphthalene (Fig. 6). The H-bond in glutarimide (XVII) is significantly longer with minimum (d_i, d_e) = (0.8, 1.15), and no evidence of very close H···H contacts, although it does display the narrow range of points typical of aliphatic H···H interactions (Fig. 3). In 6-azauracil (XVIII) each molecule accepts and donates two quite short N–H···O=C hydrogen bonds, with minimum (d_i, d_e) = (0.75, 1.1), and for this planar heterocycle there is no evidence of π···π stacking contacts.

Plots for the ring-forming amides in Fig. 10 (and including formamide in Fig. 2) contain the expected hydrogen bonding spikes and, in the cases of 1-methylthymine (XXI) and uracil (XX), a diffuse set of points in between these spikes, with shortest contact near 2.4 Å, arising once again from very close contacts across the centrosymmetric hydrogen-bonded dimer, an 8-ring in this case. The crystal structure for 1-methylthymine also contains longer C–H···O=C contacts (superimposed on the other H-bonds in Fig. 10), and there is clear evidence in the plot of C–H···π contacts. Examination of the packing diagram reveals that the hydrogen-bonded sheets are linked by methyl CH_3···π contacts, as well as by CH_3···O=C contacts. Uracil also forms sheets of molecules linked by centrosymmetric N–H···O=C rings, as well as by rings involving both N–H···O=C and C–H···O=C contacts, and both interactions overlap in the spikes in Fig. 10 for this molecule. Interlayer stacking shows up in the plot for uracil as the green to yellow region near 1.8 Å. Benzamide (XIX) also forms centrosymmetric dimers, but in this case the hydrogen bond 8-ring is

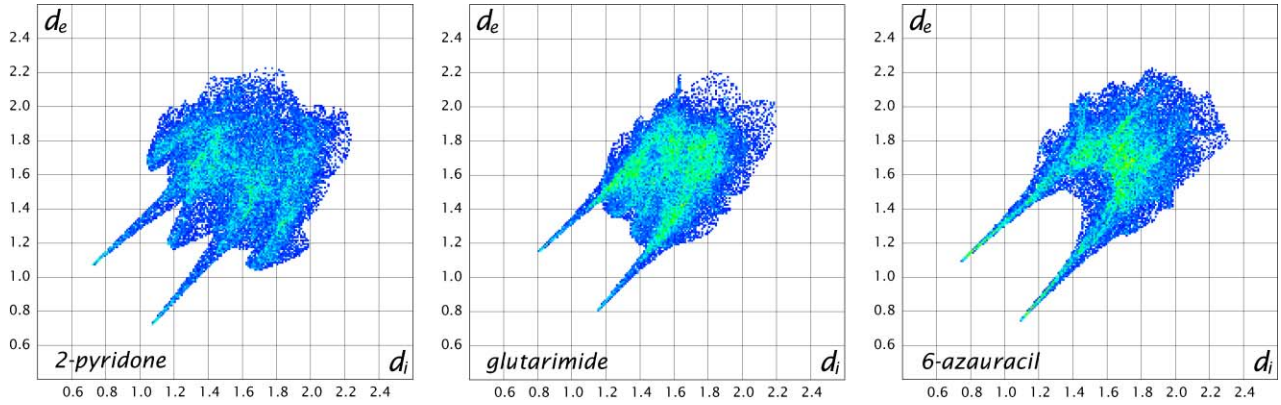

Fig. 9 2D fingerprint plots for 2-pyridone (PYRIDO04), glutarimide (GLUTIM) and 6-azauracil (AZURAC10).

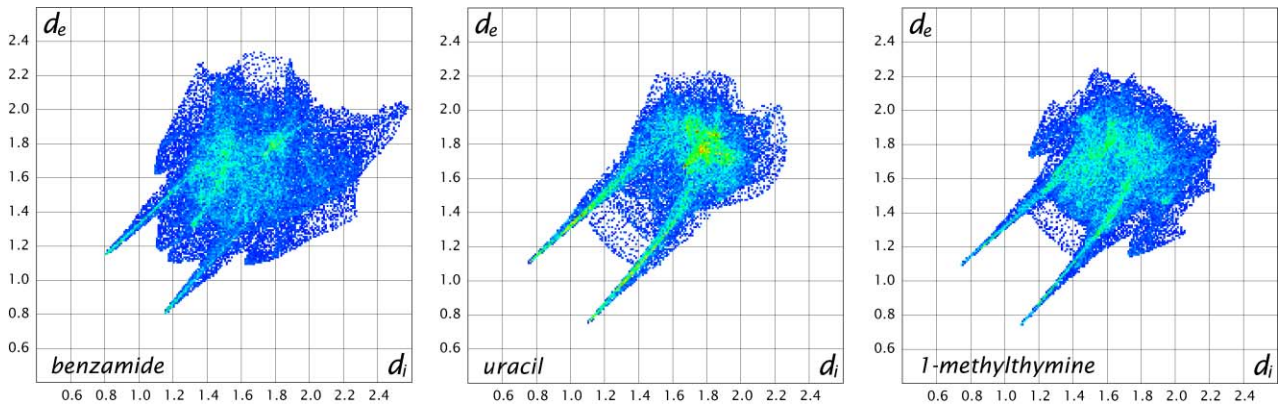

Fig. 10 2D fingerprint plots for benzamide (BZAMID03), uracil (URACIL) and 1-methylthymine (METHYM01).

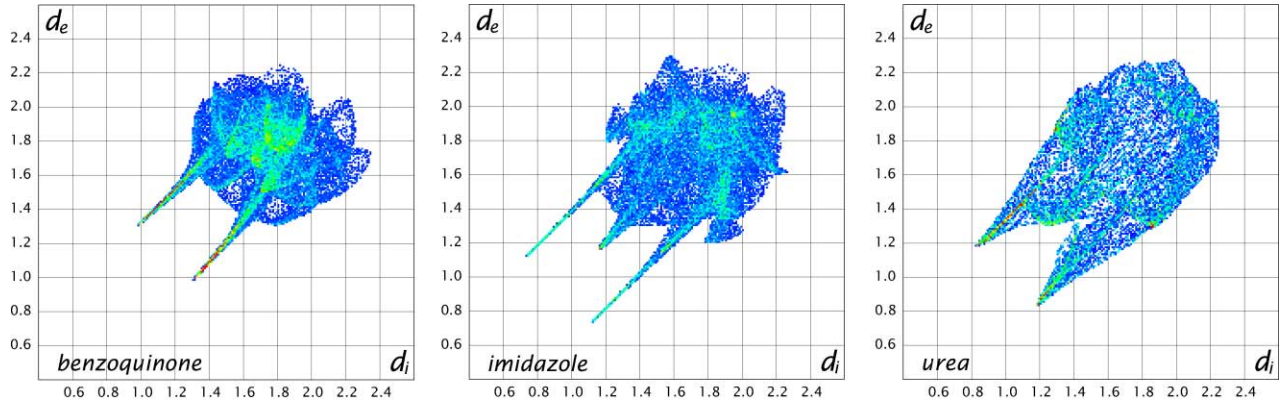

Fig. 11 2D fingerprint plots for 1,4-benzoquinone (BNZQUI02), imidazole (IMAZOL13) and urea (UREAXX14).

twisted out of the plane of the two benzene rings. The plot in Fig. 10 reveals the usual hydrogen bond features, a close C–H···π contact, and the diffuse blue tail at upper right signals a non-optimal packing between benzene rings (*i.e.* regions on the Hirshfeld surface without any close contacts to nuclei in adjacent molecules), very similar to those observed above for benzene and benzoic acid.

Miscellaneous examples of hydrogen bonding

2D plots for 1,4-benzoquinone (XXII), imidazole (XXIII), and urea (XIV) are collected in Fig. 11, for no reason other than they each display quite different hydrogen bonding patterns than already discussed above. Benzoquinone molecules form layers *via* centrosymmetric rings involving C–H···O=C contacts, and NIPMAT plots for this molecule have been presented elsewhere.[27] The relevant 2D plot in Fig. 11 displays quite clearly the dominance of the close C–H···O=C contacts (each carbonyl oxygen accepts two such weak hydrogen bonds), with characteristic hydrogen bonding 'spikes' pointing to the lower left, including a number of red points, and reaching just short of 2.3 Å. This is the only structure we have examined where the C–H···O contact is seen by itself, and it unambiguously displays the same features as other, more conventional, hydrogen bonds. We also see evidence in the plot of interplanar stacking for this crystal (the green to yellow region between 1.7 and 1.9 Å), and no sign of close contacts between H atoms. Imidazole, on the other hand, displays a H···H contact shorter than 2.4 Å (actually 2.276 Å in the original structural paper[28]), as well as the expected hydrogen bond spikes, in this case N–H···N interactions between molecules, forming ribbons in the crystal. We find it most interesting that the 2D plot in Fig. 11 also quite clearly displays the wings characteristic of a close H atom contact to the 5-ring, in this case a C–H···π contact close to 3.0 Å [*i.e.* (d_i, d_e) = (1.2, 1.8)], which was not remarked upon in the original paper.[28] McMullan *et al.* did, however, note a short intermolecular H···N distance of 2.605 Å, which appears in the plot in Fig. 11 superimposed on the hydrogen bond spikes, and is responsible for the thickening of the spikes, which occurs at 2.6 Å. We believe it is of considerable significance that what might seem to be two similar X–H···ring contacts actually appear in the fingerprint plot with either hydrogen bond or X–H···π characteristics. This is not a function of relative distances of the two contacts, but rather their orientation relative to neighbouring atoms; in one case the contact is very definitely one-on-one (and hence X–H···Y in nature) whereas in the other it is definitely one-to-many (and hence X–H···π). The final fingerprint plot in Fig. 11, that for urea, is at first sight anomalous, and without doubt utterly different from the other hydrogen-bonded materials already presented. It still displays the expected H-bond feature, with two spikes reaching down to 2.0 Å, a considerably longer distance than other N–H···O=C hydrogen bonds, and here these spikes are much broader than any encountered so far. This difference results from the exceptional capacity of the carbonyl oxygen atom in urea to accept four hydrogen bonds, two each of two different geometries, and hence each H-bond is somewhat weaker than we have seen elsewhere, and the geometry far from the preferred near-linear H···O=C orientation. All of these differences conspire to produce a quite different and greatly broadened pattern in the fingerprint plot, and we will see a similar feature below in one form of oxalic acid.

For our final example of hydrogen-bonded structures we have chosen the series of 2-, 3- and 4-aminophenols discussed in detail recently by Allen *et al.*,[29] with a focus on the unusual mutual recognition pattern found in 2- and 3-aminophenol, compared to that observed in 4-aminophenol. The fingerprint plots (Fig. 12) are immediately seen to be rather different from those already encountered. All three structures exhibit

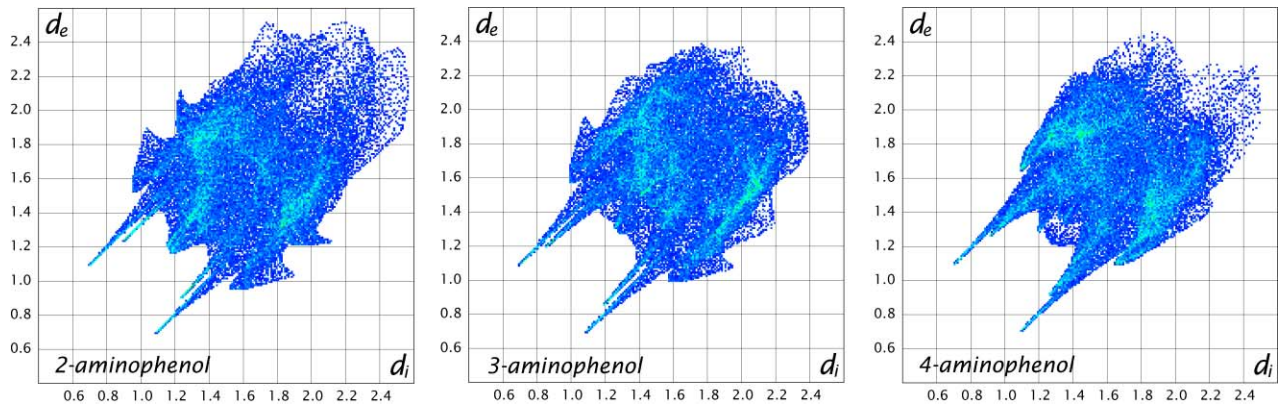

Fig. 12 2D fingerprint plots for 2-aminophenol (AMPHOM03), 3-aminophenol (MAMPOL02) and 4-aminophenol (AMPHOL01).

two quite distinct hydrogen bonds, as evidenced by the appearance of two pairs of H-bond spikes. The longer of these corresponds to the closer O–H···N hydrogen bond (near 1.8 Å in all three crystal structures), while the shorter spike corresponds to the more distant N–H···O hydrogen bond (near 2.15 Å in 2-aminophenol, 2.05 Å in 3-aminophenol, and 2.20 Å in 4-aminophenol). The existence of X–H···π contacts is clear from the 'wings' in plots for 2- and 3-aminophenol, just as their absence in 4-aminophenol is equally clear. 2-Aminophenol actually displays features expected of two different X–H···π contacts, a close one near 2.4 Å (N–H···π in this case), and a more distant one near 3.0 Å (C–H···π); 3-aminophenol displays an N–H···π contact nearer 2.5 Å, and this is borne out by the relevant close contacts in the original paper.[29] These fingerprint plots rapidly convey the significant differences and similarities between this series of related structures, and it would seem to us that they would be a useful complement to more conventional tools (such as tables of close intermolecular contacts, and crystal packing diagrams) in comparisons of the sort attempted by Allen *et al.*

Contacts involving halogens

As discussed in some detail by Desiraju,[15,16] crystal structures of molecules containing the halogens chlorine, bromine and iodine are characterised by short, non-bonded contacts, and there has been some debate about the nature of these interactions, with Desiraju and others maintaining that they result from specific attractive forces,[30] while Price *et al.* have concluded on the basis of crystal data and theoretical calculations that they are manifestations of the packing of anisotropic atoms.[31] The interaction clearly involves the polarizability of these atoms, but we make no attempt here to delve further into the origin of this phenomenon. As above, we aim merely to illustrate the features in fingerprint plots that arise from observed crystal structures, and for this purpose confine our attention to molecules containing chlorine.

Fig. 13 presents the fingerprint plots for Cl_2 and five different chlorinated hydrocarbons. The plot for molecular chlorine[32] reveals an exceptionally small range of Cl···Cl contacts, ranging from a shortest approach of roughly 3.3 Å, and it is noticeable that the distribution of points between (1.65, 1.65) and (1.85, 1.85) is very narrow, while beyond that it broadens considerably, although the striking red stripe indicates the vast majority of contacts fall within a small range. We suspect that it is not a coincidence that the generally accepted van der Waals radius for Cl is near 1.75 Å; above this the pattern of points in the fingerprint plot suggests isotropic van der Waals contacts, while below this the pattern is extremely narrow, and actually closely resembles the hydrogen bond spikes (although now between like atoms, and hence appearing on the diagonal). All of this hints at some intermolecular contacts in Cl_2 being different from, and not just closer than, others. Along the same lines we note that the plots for carbon tetrachloride and hexachlorobenzene in Fig. 13 do not contain contacts below (1.75, 1.75); these crystals would appear to contain van der Waals interactions rather than specific Cl···Cl attractive forces as appear in Cl_2.

The changing appearance in the fingerprint plots on reducing the chlorine content of the chloromethanes from CCl_4 to CH_3Cl is rather fascinating. Chloroform displays a Cl···Cl pattern similar to CCl_4, but also very obvious 'wings' due to quite specific C–H···Cl contacts at around 2.95 Å. The characteristic Cl···Cl contact pattern is also evident in the plot for dichloromethane, although it is a much less significant feature here (*i.e.* relatively fewer contacts of this kind in this structure); the C–H···Cl contact also appears for this structure near 3.0 Å, and now there is also evidence of a small number of points involving H···H contacts, but only as close as 2.7 Å (the diffuse pattern of blue points between the 'wings').

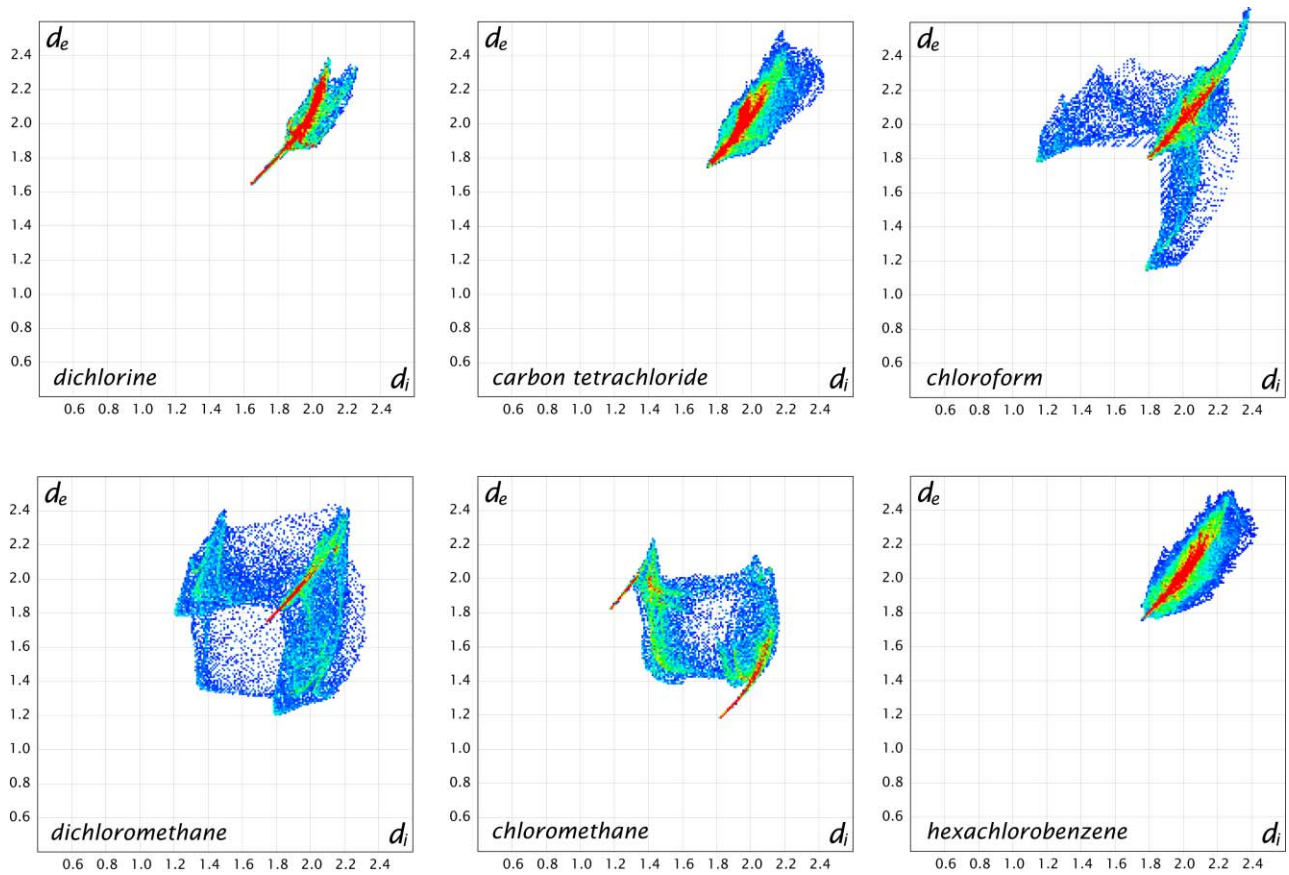

Fig. 13 2D fingerprint plots for chlorine (ref. 32), carbon tetrachloride (CARBTC), chloroform (CLFORM), dichloromethane (DCLMET10), chloromethane (CLMETH) and hexachlorobenzene (HCLBNZ11).

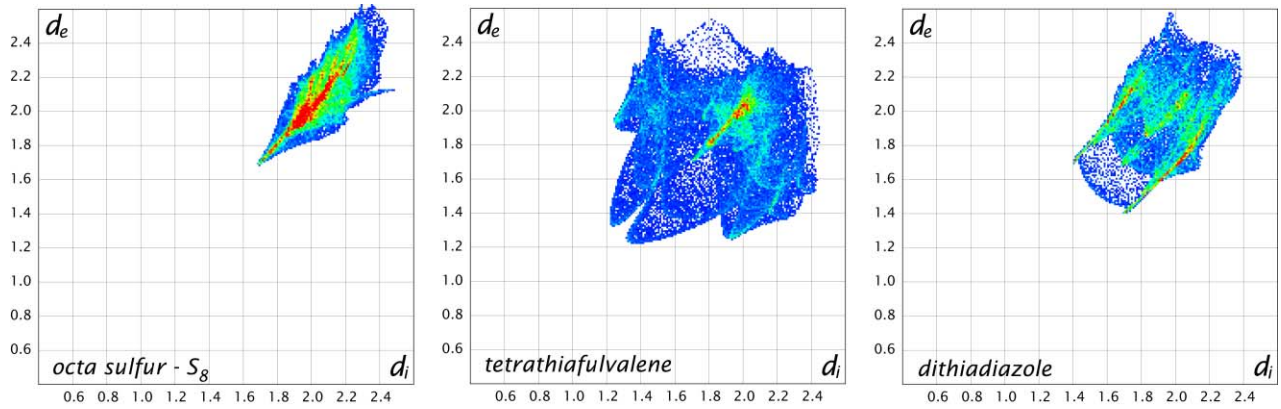

Fig. 14 2D fingerprint plots for cyclic S_8 (FURHUV), tetrathiafulvalene (BDTOLE10) and dithiadiazole [(1,2,5)-thiadiazole-(3,4-*c*)(1,2,5)-thiadiazole] (BAWHEM).

Finally, the plot for chloromethane shows that there are no Cl···Cl contacts in this structure, as well as a considerably greater fraction of H···H contacts. Instead it appears to be dominated by a striking C–H···Cl contact near 3.0 Å, and this feature strongly resembles that observed repeatedly for hydrogen bonding. We make no attempt to claim that this feature is evidence for a C–H···Cl hydrogen bond, but we anticipate that the similarity noted above is not coincidental, and note that convincing evidence for not only the existence, but also for the common occurrence, of C–H···Cl hydrogen bonds has been presented recently.[33]

Contacts involving sulfur

As for the halogens, sulfur is known to form close intermolecular contacts of the kind S···S, S···N and S···Cl, with quite specific directional preferences as demonstrated by Parthasarathy and co-workers.[34] Fig. 14 illustrates three examples. The range of S···S contacts evident in the plot for S_8 is limited, the shortest being near 3.4 Å, and the broad features are remarkably similar to those observed for CCl_4 and C_6Cl_6 in Fig. 13, but not precisely as for Cl_2. Tetrathiafulvalene (TTF, XXV in Chart 2) displays similar S···S contacts, especially beyond 3.6 Å in the plot, arising from neighbouring molecules above, below and to the side, but also broad 'wings' due to two C–H···S contacts at roughly 3.2 Å, some evidence of interlayer stacking near (1.8, 1.8), overlapping with the S···S contacts for this molecule (it could of course be argued that the S···S contacts determine the interlayer spacing), and a substantial number of points reaching down to (1.2, 1.2), and arising from the closest H···H contacts in the structure. The latter feature is bifurcated, and we tentatively attribute this to the fact that the H···H contact here is not one-on-one. The final plot in Fig. 14 is for dithiadiazole (XXVI), a molecule devoid of H atoms. The relevant contacts evident in the plot include S···S and interlayer (near 1.8 Å and upwards), although these are not the dominant features here. Instead, we see two sharp spikes reaching down towards the lower left, with a diffuse pattern of blue points in between. This is reminiscent of the cyclic hydrogen bond patterns in Figs. 8 and 10, and in this case it arises from close, and quite specific, S···N contacts forming a cyclic 4-ring. This interaction has been the subject of a recent charge density study on S_4N_4 by Scherer *et al.*,[35] who quite convincingly demonstrated the existence of charge concentrations around S and N atoms responsible for this characteristic molecular recognition motif.

Polymorphs and crystal structures with $Z' > 1$

Crystalline polymorphism has always attracted considerable attention, and recent studies include those by Gavezzotti and Filippini,[36] Caira,[37] and Sarma and Desiraju.[38] Very early in our study of Hirshfeld surfaces, we were aware of their potential in the study of polymorphism of molecular materials, as well as crystal structures with more than one molecule in the asymmetric unit ($Z' > 1$). This is a direct consequence of the uniqueness of Hirshfeld surfaces for any given crystal structure, and as examples we presented Hirshfeld surfaces for polymorphic structures of oxalic acid and 1,4-dichlorobenzene.[4] Here we pursue those same materials, although we could choose from many other possibilities as well; as above, we aim to present examples, rather than to make any attempt at comprehensiveness.

Fingerprint plots for the α and β forms of anhydrous oxalic acid are given in Fig. 15. Hirshfeld surfaces for the α and β forms of oxalic acid are dramatically different (see Fig. 9 of ref. 4), and show quite effectively the different packing modes utilized in the two structures. Interestingly, the volumes of these two surfaces are identical, and the surface area of the α

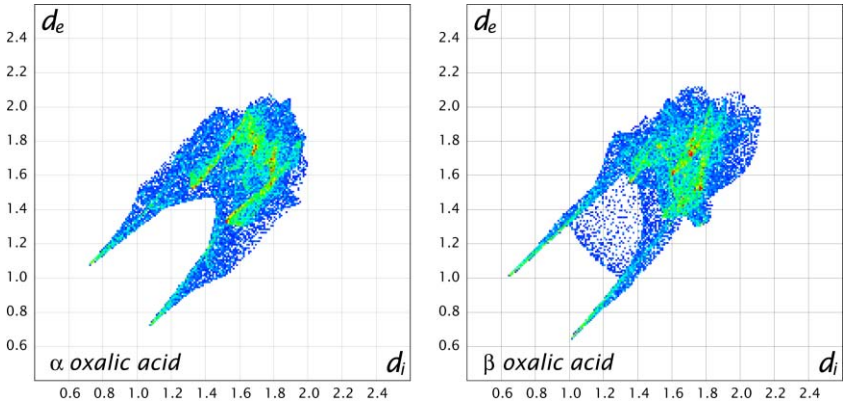

Fig. 15 2D fingerprint plots for α (OXALAC05) and β (OXALAC04) anhydrous oxalic acid.

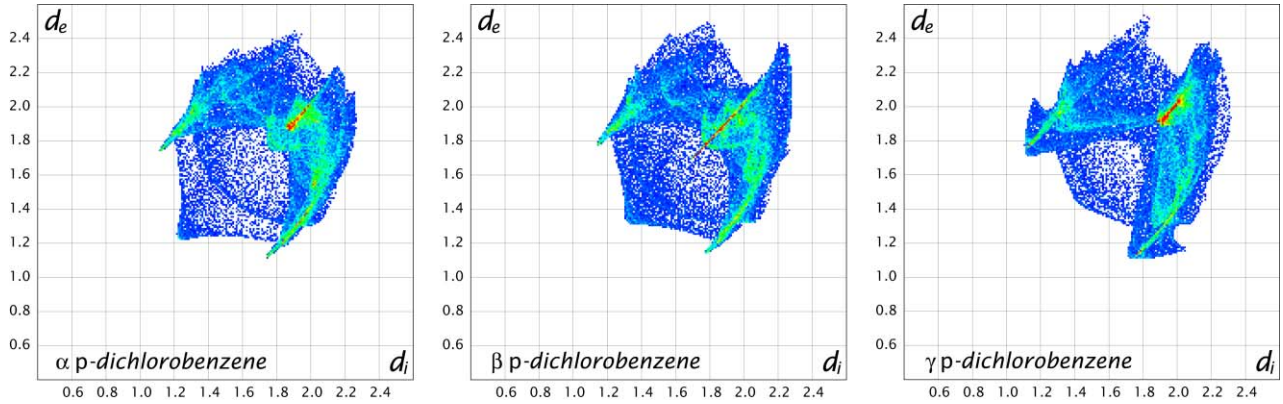

Fig. 16 2D fingerprint plots for α (DCLBEN07), β (DCLBEN05) and γ (DCLBEN03) polymorphs of 1,4-dichlorobenzene.

form is somewhat greater than that of the β form. α-Oxalic acid crystallizes with a strong three-dimensional network of hydrogen bonds and close contacts, essentially a pseudo-fcc arrangement, somewhat similar to that in benzene. The fingerprint plot suggests that this lack of a single, strong, directional O–H···O=C hydrogen bond is compensated by the presence of many slightly weaker interactions, as the characteristic H-bond spikes are now markedly broadened, in much the same way as observed for urea (Fig. 11). The 2D plot for the β polymorph shows evidence of the strong O–H···O=C interactions at each end of the centrosymmetric molecule, and the overall plot strongly resembles those for other ring-forming carboxylic acids in Fig. 8.

Polymorphism in 1,4-dichlorobenzene formed part of the recent crystallographic and computational study of dichlorobenzenes by Boese *et al.*[39] Hirshfeld surfaces for the three crystalline polymorphs reveal a similarity between molecular shapes for the α and β forms, and the distinctly different packing in the γ polymorph.[4] Fingerprint plots (Fig. 16) confirm these similarities and differences, and enable us to illuminate them further. All three display the expected Cl···Cl contacts, and it is obvious that the closest such contact is near 3.7 Å [*i.e.* from (1.85, 1.85) upwards] for the α and γ forms, but there is a much closer contact in the β form, as evinced by the very sharp red line along the diagonal starting near (1.7, 1.7), suggesting a closest Cl···Cl contact of 3.4 Å. Moreover, because this feature is so sharp and thin, the relevant contact must be virtually head-to-head (linear C–Cl···Cl–C); this is confirmed in the original structural studies.[40] However, whereas the emphasis in previous discussions of crystal packing in these materials has focused almost entirely on Cl···Cl contacts, they tell only a part of the story. All three polymorphs in Fig. 16 display relatively distant C–H···Cl contacts, as seen by the sharp spikes approaching (1.1, 1.7) in the plots, and hence a closest contact near 2.8 Å, considerably shorter than observed for the chloromethanes (Fig. 13). This pattern for the γ form is superimposed on the quite obvious 'wings' arising from a C–H···π contact which occurs only in this polymorph. Blue points located between the C–H···Cl spikes are due to the closest H···H contacts in the structures, and it is clear that the α form has considerably closer H···H contacts than the other two forms.

Steiner has recently summarized the frequencies of occurrence of structures with $Z' > 1$, and observed that for organic molecules only 10.8% of CSD structures have $Z' > 1$, and of those only 0.6% have $Z' > 3$. We provide a single example of a molecular crystal with $Z' > 1$ in Fig. 17, namely aziridine (XXVII in Chart 2), for which $Z' = 3$, which results in three different pairs of enantiomeric Hirshfeld surfaces for this centrosymmetric space group. The most conspicuous feature of the structure is the chains of N–H···N hydrogen bonds proceeding in opposite directions along the *b* axis. These chains link molecules 3, 2 and 1 in a donor···acceptor sequence, with all N–H groups facing inwards. The hydrogen bonds are quite weak and this is reflected in the fingerprint plots, where all hydrogen-bonded spikes are noticeably short (compare these plots with that for benzoquinone in Fig. 11), corresponding to N–H···N contacts greater than 2.1 Å. For molecules 1 and 3 the N–H···N contact is only slightly closer than the closest H···H contact (the sharp spike between the H-bond features, suggesting H···H distance near 2.2 Å for both molecules). Molecule 2 quite clearly has no close H···H contacts, and this in itself is worthy of note. Whereas in all other examples of fingerprint plots above, where there was only a single molecule in the asymmetric unit, and hence all intermolecular contacts were reflected in a single Hirshfeld surface, and hence a single fingerprint plot, here we see that we may need to inspect more than one plot to see a complete interaction. As an example, we note that not all H-bond spikes in Fig. 17 are identical. Careful inspection reveals that the

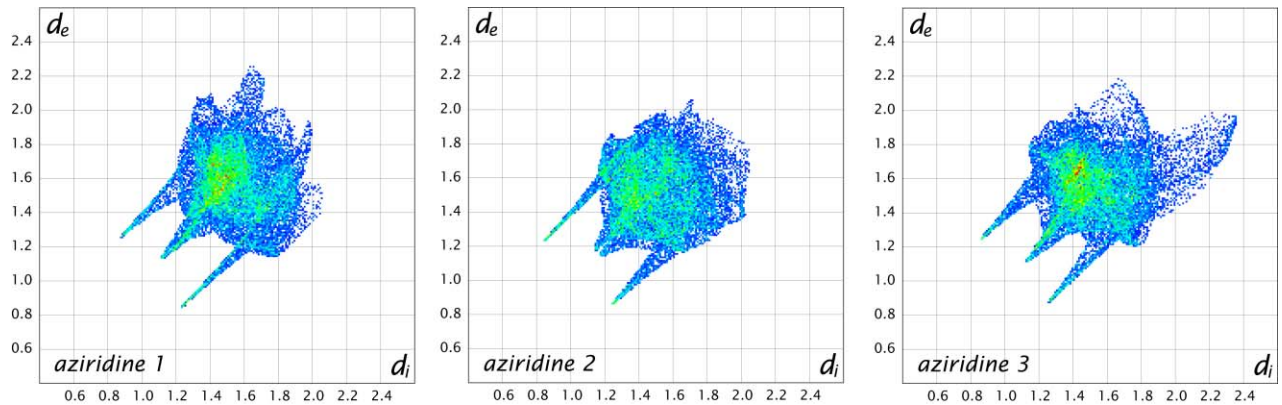

Fig. 17 2D fingerprint plots for the three different molecules in the crystal structure of aziridine (NEBPUF).

spike at the lower right for molecule 1 is longer and narrower than that at the upper left, evidence that the donor and acceptor molecules are not the same for these two interactions. The spike at the lower right for molecule 1 is the acceptor part of an interaction; the complementary donor part is found at the upper left of the plot for molecule 2, and we see that this particular N–H···N hydrogen bond goes from molecule 2 to molecule 1. There are other subtle but important differences that emerge from these plots. The Hirshfeld volume[41] indicates that molecule 2 has a more crowded environment than the other two molecules, and this is apparent in the fingerprint plots by the number of points at quite large distances for molecules 2 and 3, compared with the relatively compact pattern for molecule 2.

Conclusions

There were many, many examples for us to choose from in the course of compiling this work, and we have had to be highly selective in order to show as much as possible in this rather brief communication. There seems little doubt that the Hirshfeld surface, along with the 2D fingerprint plots presented for the first time in this paper, is providing information that cannot be obtained from conventional crystal packing diagrams or by detailed consideration of close intermolecular contacts, and we firmly believe that these tools will form a useful complement to the more traditional means of discussing, comparing and elucidating patterns in intermolecular interactions in crystals. Although our focus here has been entirely on the 2D fingerprint plots, we will be presenting detailed studies elsewhere which incorporate the actual surfaces themselves, with various functions mapped on them, and it is clear to us that this approach extracts the most information from these intriguing objects.

In the course of developing this tool and writing this paper, ideas for rather obvious extensions of the fingerprint plot approach came to mind. These include the decomposition of 2D plots into specific atom–atom pairs, or even group–group interactions, and perhaps the utilization of angular information as well as the present distances. Developments of this kind await the incorporation of our tools into software which interfaces more directly with the CSD. We believe that Hirshfeld surfaces in their various guises, combined with the enormous power of the CSD, will comprise a formidable armoury to use in future attempts to understand and rationalise interactions in molecular crystals, and eventually to design materials with predictable structures and desired physical properties. As noted by Bartlett thirty years ago,[42] ''there are times when the shortest route to the new is a determined attempt to understand what is known''.

Notes and references

1 G. R. Desiraju and T. Steiner, *The Weak Hydrogen Bond*, Oxford University Press, 1999.
2 A. Nangia and G. R. Desiraju, in *Design of Organic Solids*, E. Weber, ed., Springer-Verlag, Berlin, 1998, p. 87.
3 M. A. Spackman and P. G. Byrom, *Chem. Phys. Lett.*, 1997, **267**, 215.
4 J. J. McKinnon, A. S. Mitchell and M. A. Spackman, *Chem. Eur. J.*, 1998, **4**, 2136.
5 F. H. Allen and O. Kennard, *Chem. Des. Automat. News*, 1993, **8**, 31 (www.ccdc.cam.ac.uk).
6 It is important to recognise that the use of spherical electron densities does not assume anything about the electron distribution in either the molecule or the crystal, which is well known to be anisotropic about each nucleus. The spherical electron distributions at each atomic site are the basis of Hirshfeld's stockholder partitioning scheme, but they also result in relatively trivial computations to determine the isosurface.
7 All crystal structures are taken from the CSD October 2001 release. The weight function is defined using Hartree–Fock atomic electron densities (E. Clementi and C. Roetti, *At. Data Nucl. Data Tables*, 1974, **14**, 177), contracted hydrogen atoms ($\zeta = 1.24$), and X–H bond lengths fixed at average neutron diffraction values (F. H. Allen, O. Kennard, D. G. Watson, L. Brammer, A. G. Orpen and R. Taylor, in *International Tables for Crystallography*, A. J. C. Wilson, ed., Kluwer Academic, Dordrecht, 1995, p. 685). Triangulation was performed with the marching cubes algorithm (W. E. Lorenson and H. E. Cline, *Comput. Graphics*, 1987, **21**, 163; W. Heiden, T. Goetze and J. Brickmann, *J. Comput. Chem.*, 1993, **14**, 246) with a grid resolution of 0.2 Å.
8 All closest contacts within the same range of d_e and d_i are binned together, irrespective of the nature of the atoms involved.
9 To facilitate comparison between molecules of quite different sizes, and hence surface areas, colours are determined by the fraction of surface points in each bin. Actual colours span a continuous range, and are mapped using the HSV scheme, where $S = V = 1.0$, and $H = 0.66$ (240°, blue) for minimum relative area, and $H = 0.0$ (0°, red) for more than 0.1% of surface points in the bin.
10 R. S. Rowland, *Am. Crystallogr. Assoc. Abstr.*, 1995, 63.
11 G. R. Desiraju, *Chem. Commun.*, 1997, 1475.
12 G. R. Desiraju, *Acc. Chem. Res.*, 1996, **29**, 441.
13 S. L. Price and K. S. Wibley, *J. Phys. Chem. A*, 1997, **101**, 2198.
14 L. Fabian, G. Argay and A. Kalman, *Acta Crystallogr., Sect. B*, 1999, **55**, 788.
15 G. R. Desiraju, *Crystal Engineering: The Design of Organic Solids*, Elsevier, Amsterdam, 1989.
16 G. R. Desiraju and C. V. K. Sharma, in *The Crystal as a Supramolecular Entity*, G. R. Desiraju, ed., Wiley, Chichester, 1996, p. 31.
17 See Table 1.6, p. 15 of ref. 1.
18 R. Boese, H. C. Weiss and D. Bläser, *Angew. Chem., Int. Ed.*, 1999, **38**, 988; V. R. Thalladi and R. Boese, *New J. Chem.*, 2000, **24**, 579.
19 The trend of melting point with increasing number of C atoms is not smoothly monotonic; members of the series with an even number of C atoms have melting points that are relatively higher than those of the molecules with odd numbers. Furthermore, propane has the lowest melting point of all the *n*-alkanes.
20 For example, see Table 1.8 of ref. 1, which contains values due to Bondi (A. Bondi, *J. Phys Chem.*, 1964, **68**, 441). Similar values were recently obtained from a re-analysis of crystallographic data (R. S. Rowland and R. Taylor, *J. Phys Chem.*, 1996, **100**, 7384), except the radius for H was found to be nearer 1.1 Å, a value more in line with the fingerprint plots presented here.
21 We also produced fingerprint plots for other *n*-butane structures reported in the CSD: DUCKOB (5 K), DUCKOB01 (90 K), DUCKOB02 (65 K) and DUCKOB03 (120 K). These structures all derive from neutron powder diffraction experiments (K. Refson and G. S. Pawley, *Acta Crystallogr., Sect. B*, 1986, **42**, 402), and span all three known forms of *n*-butane. In all cases the 2D fingerprint plots are dramatically different from that in Fig. 3, and all structures result in apparently unrealistically short H···H contacts (as short as 1.92 Å for DUCKOB02 and DUCKOB03). This exercise convinced us of the general utility of our 2D plots to rapidly compare structures and even identify unexpected (and perhaps unrealistic) intermolecular contacts.
22 G. R. Desiraju and A. Gavezzotti, *Acta Crystallogr., Sect. B*, 1989, **45**, 473.
23 J. D. Dunitz and A. Gavezzotti, *Acc. Chem. Res.*, 1999, **32**, 677.
24 C. A. Hunter and J. K. M. Sanders, *J. Am. Chem. Soc.*, 1990, **112**, 5525; J. F. Malone, C. M. Murray, M. H. Charlton, R. Docherty and A. J. Lavery, *J. Chem. Soc., Faraday Trans.*, 1997, **93**, 3429; C. A. Hunter, K. R. Lawson, J. Perkins and C. J. Urch, *J. Chem. Soc., Perkin Trans. 2*, 2001, 651.
25 See, for example, relevant chapters in ref. 15, as well as E. Weber, *Design of Organic Solids*, Springer-Verlag, Berlin, 1998, and G. R. Desiraju, *The Crystal as a Supramolecular Entity*, Wiley, Chichester, 1996.
26 T. Steiner, *Angew. Chem., Int. Ed.*, 2002, **41**, 48.
27 See Fig. 2.38 of ref. 1, or Fig. 4 of ref. 12.
28 R. K. McMullan, J. Epstein, J. R. Ruble and B. M. Craven, *Acta Crystallogr., Sect. B*, 1979, **35**, 688.
29 F. H. Allen, V. J. Hoy, J. A. K. Howard, V. R. Thalladi, G. R. Desiraju, C. C. Wilson and G. J. McIntyre, *J. Am. Chem. Soc.*, 1997, **119**, 3477.
30 G. R. Desiraju and R. Parthasarathy, *J. Am. Chem. Soc.*, 1989, **111**, 8725.
31 S. L. Price, A. J. Stone, J. Lucas, R. S. Rowland and A. E. Thornley, *J. Am. Chem. Soc.*, 1994, **116**, 4910.
32 E. D. Stevens, *Mol. Phys.*, 1979, **37**, 27.
33 C. B. Aakeröy, T. A. Evans, K. R. Seddon and I. Pálinkó, *New J. Chem.*, 1999, **23**, 145.

34 R. E. Rosenfield, R. Parthasarathy and J. D. Dunitz, *J. Am. Chem. Soc.*, 1977, **99**, 4860; T. N. Guru Row and R. Parthasarathy, *J. Am. Chem. Soc.*, 1981, **103**, 477.
35 W. Scherer, M. Spiegler, B. Pedersen, M. Tafipolsky, W. Hieringer, B. Reinhard, A. J. Downs and G. S. McGrady, *Chem. Commun.*, 2000, 635.
36 A. Gavezzotti and G. Filippini, *J. Am. Chem. Soc.*, 1995, **117**, 12 299.
37 M. R. Caira, in *Design of Organic Solids*, E. Weber, ed., Springer, Berlin, 1998, p. 163.
38 J. A. R. P. Sarma and G. R. Desiraju, in *Crystal Engineering. The Design and Application of Functional Solids*, K. R. Seddon and M. Zaworotko, ed., Kluwer Academic, Amsterdam, 1999, p. 325.
39 R. Boese, M. T. Kirchner, J. D. Dunitz, G. Filippini and A. Gavezzotti, *Helv. Chim. Acta*, 2001, **84**, 1561.
40 G. L. Wheeler and S. D. Colson, *J. Chem. Phys.*, 1976, **65**, 1227.
41 The relevant volumes inside the Hirshfeld surfaces for these three molecules are 67.4, 63.7 and 65.5 $Å^3$, for molecules 1, 2, and 3, respectively.
42 P. D. Bartlett, *J. Am. Chem. Soc.*, 1972, **94**, 2161.